International Journal of Mathematical Archive-7(9), 2016, 98-111
Available online through www.ijma.info ISSN 2229 – 5046

COMBINED EFFECTS OF CHEMICAL REACTION, DUFOUR, SORET EFFECTS ON UNSTEADY MHD FLOW PAST AN IMPULSIVELY STARTED INCLINED POROUS PLATE WITH VARIABLE TEMPERATURE AND MASS DIFFUSION

M. ANIL KUMAR[1*], Y. DHARMENDAR REDDY[1]

**[1]Department of Mathematics,
Anurag Group of Institutions, Venkatapur, Ghatkesar, RR District, Telangana, India.**

(Received On: 08-08-16; Revised & Accepted On: 08-09-16)

ABSTRACT

T*he aim of this research paper is to study the combined effects of Soret, Dufour on an unsteady MHD flow past an infinite vertical plate in a porous medium with variable temperature and mass diffusion in presence of chemical reaction. The momentum, energy, and concentration equations derived as coupled second-order, ordinary differential equations and are solved numerically using a highly accurate and thoroughly tested finite element method (FEM). The effects of Soret number, Dufour number, Grashof number for heat and mass transfer, Schmidt number, Chemical reaction parameter, Prandtl number and Permeability parameter on the dimensionless velocity, temperature and concentration profiles are presented graphically. In addition the local values of the Skin –friction coefficient, Nusselt number and Sherwood number are also shown in tabular form. The discussion focuses on the physical interpretation of the results as well their comparison with the results of previous studies*

Keywords: *MHD, Heat Transfer, Mass Transfer, Porous Medium and Finite Element Method.*

1. INTRODUCTION

Radiative convective flows have gained attention of many researchers in recent years, Radiation plays a vital role in many engineering, environment and industrial process example, heating and cooling chambers, fossil fuel combustion energy process astrophysical flow and space vehicle re-entry. Alagoa *et. al* [1] analyzed the effect of radiation on free convective MHD flow through a porous medium between infinite parallel plates in the presence of time dependent suction. The unsteady free convective flow with radiation effect was investigated by Cogley *et. al* [2]. Rajput and Sahu [3] have investigated effects of rotation and magnetic field on the flow past an exponentially accelerated vertical plate with constant temperature. Soundalgekar and Wavre [4] studied an unsteady free convection flow past an infinite vertical plate with constant suction and Mass transfer. Unsteady MHD free convection flow past an infinite vertical plate with Soret, Dufour thermal radiation and heat source has been studied by Anand Rao *et.al* [5]. Due to the importance of Soret and Dufour effects for the fluids with very light molecular weight as well as medium molecular weight many investigators have studied and reported results for these flows of whom the names are Eckert and Drake [6], Durusukanya and Worek [7].Very recently, Alam and Rahman [8] studied the Dufour and Soret effects on steady MHD free convective heat and mass transfer flow past an semi-infinite vertical porous plate embedded in a porous medium. Soret Dufour and radiation effects on unsteady MHD flow past an impulsively started inclined porous plate with variable temperature and mass diffusion has been studied by Pandya and Shukla [9].

The objective of this paper is to investigate the combined effects Chemical reaction, Soret, Dufour and Thermal Radiation on an inclined porous vertical plate in presence of variable temperature and concentration. The governing equations are solved using Galerkin method. The effect of different physical parameters on velocity, temperature and concentration are discussed and presented graphically.

The governing equations are solved using Galerikan method. The effect of different physical parameters on velocity, temperature and concentration are discussed and presented graphically.

***Corresponding Author: M. Anil Kuma[1*], [1]Department of Mathematics,
Anurag Group of Institutions, Venkatapur, Ghatkesar, RR District, Telangana, India.***

2. MATHEMATICAL ANALYSIS

The unsteady flow of a viscous incompressible electrically conducting fluid past an impulsively started infinite inclined porous plate with variable temperature and mass diffusion in presence of radiation is considered. The plate is inclined at angle α to vertical, is embedded in porous medium. The x^* - axis is taken along the plate and y^*-axis is taken normal to it. It is also assumed that the radiation heat flux in x^*-direction is negligible as compared to that in y^*-direction initially. The plate and fluid are at the same temperature and concentration. At time the plate is given impulsive motion along x^*-direction against gravitational field with constant velocity u_0, the plate temperature and concentration decrease exponentially with time. The transversely applied magnetic field and magnetic Reynolds numbers are very small and hence induced magnetic field is negligible. Due to infinite length in x^*-direction, the flow variables are functions of y^* and t^* only. Under the usual Boussinesq approximation, governing equations for this unsteady problem are given by:

Continuity equation:

$$\frac{\partial v^*}{\partial y^*} = 0 \Rightarrow v^* = -v_0 \tag{1}$$

Momentum equation:

$$\frac{\partial u^*}{\partial t^*} + v^* \frac{\partial u^*}{\partial y^*} = \nu \frac{\partial^2 u^*}{\partial y^{*2}} + g\beta(T^* - T_\infty^*)\cos(\alpha) + g\beta'(C^* - C^*_\infty)\cos(\alpha) - \frac{\sigma {B_O}^2 u^*}{\rho} - \frac{\nu u^*}{K^*} \tag{2}$$

Energy equation:

$$\rho C_p \left\{ \frac{\partial T^*}{\partial t^*} + v^* \frac{\partial T^*}{\partial y^*} \right\} = k \frac{\partial^2 T^*}{\partial y^{*2}} - \frac{\partial q_r}{\partial y^*} + \frac{\rho D_m K_T}{c_s} \frac{\partial^2 C^*}{\partial y^{*2}} \tag{3}$$

Concentration equation:

$$\frac{\partial C^*}{\partial t^*} + v^* \frac{\partial C^*}{\partial y^*} = D \frac{\partial^2 C^*}{\partial y^{*2}} + \frac{D_m K_T}{T_m} \frac{\partial^2 T^*}{\partial y^{*2}} - K_r^* (C^* - C^*_\infty) \tag{4}$$

Where u^* and v^* are the Velocity components along x^*-direction and y^*-direction respectively. g is the acceleration due to gravity, β is the volumetric coefficient of thermal expansion, β' is the coefficient of volume expansion for mass transfer, ν is the kinematic viscosity, ρ is the fluid density, B_o is magnetic induction, K^* is the permeability of porous medium, σ is the electrical conductivity of the fluid, T^* is the dimensional temperature, T_∞^* is temperature of free stream C_∞^* is concentration of free stream, D_m is the chemical molecular diffusivity, k is the thermal conductivity of the fluid, C_p is specific heat at constant pressure, K_T is thermal diffusion ratio, C^* is the dimensional concentration, q_r is radiative heat flux in y^* direction, T_m is mean fluid temperature, K_r is the chemical reaction parameter.

The initial and boundary conditions are:

$$\begin{aligned}
&t^* \le 0 \quad u^* = 0 \quad T^* = T_\infty^* \quad C^* = C_\infty^* \quad \forall y^* \\
&t^* \ge 0 \quad u^* = u_0 \quad T^* = T_\infty^* + (T_w^* - T_\infty^*)e^{-At^*} \\
&C^* = C_\infty^* + (C_w^* - C_\infty^*)e^{-At^*} \text{ at } \quad y^* = 0 \\
&u^* = 0 \quad T^* \to T_\infty^* \quad C^* \to C_\infty^* \quad y^* \to \infty
\end{aligned} \tag{5}$$

Here $A = \frac{v_0^2}{V}$, C^*_w and T^*_w are concentration and temperature of plate respectively.

The radiative heat flux term by using Rosseland approximation is given by

$$q_r = -\frac{4\sigma}{3k_1}\frac{\partial T^{*4}}{\partial y^*} \tag{6}$$

Where k_1 and σ are mean absorption coefficient and Stefan Boltzmann constant respectively.

It is assumed that the temperature difference within the flow are sufficiently small such that T^{*4} may be expressed as a linear function of the temperature this is accomplished by expanding in a Taylor series about T_∞ and neglecting the higher order terms, thus

$$T^{*4} \cong 4T_\infty^{*3} T^* - 3T_\infty^{*4} \tag{7}$$

Then using (6) and (7) in equation (3), is reduced

$$\rho C_p\left\{\frac{\partial T^*}{\partial t^*} + \nu^*\frac{\partial T^*}{\partial y^*}\right\} = k\frac{\partial^2 T^*}{\partial y^{*2}} + \frac{16\sigma T_\infty^{*3}}{3k1}\frac{\partial^2 T^*}{\partial y^{*2}} + \frac{\rho D_m K_T}{c_s}\frac{\partial^2 C^*}{\partial y^{*2}} \tag{8}$$

On introducing non dimensional quantities:

$$u=\frac{u^*}{u_o},\ t=\frac{t^* v_o^{\,2}}{\nu},\ y=\frac{y^* v_0}{\nu},\ \theta=\frac{T^*-T_\infty^*}{T_w^*-T_\infty^*},\ C=\frac{C^*-C_\infty^*}{C_w^*-C_\infty^*},\ Gm=\frac{\nu g\beta'(C_w^*-C_\infty^*)}{u_0 v_0^{\,2}},$$

$$Gr=\frac{\nu g\beta(T_w^*-T_\infty^*)}{u_0 v_0^{\,2}},\ K=\frac{v_0^2 K^*}{\nu^2},\ Pr=\frac{\rho c_p \nu}{k},\ M=\frac{\sigma B_0^2 \nu}{\rho v_0^2},\ Du=\frac{D_m K_T(C_w^*-C_\infty^*)}{c_s C_p \nu(T_w^\infty-T_\infty^*)},\ Sc=\frac{\nu}{D},$$

$$Sr=\frac{D_m K_T(T_w^*-T_\infty^*)}{T_m\nu(C_w^*-C_\infty^*)},\ R=\frac{4\sigma T_*^3}{k_1 k},\ K_r=\frac{K_r^*\nu}{v_0^2} \tag{9}$$

By virtue of equation (9) we get the following governing equations which are non-dimensional form of equations (2), (3) and (8) respectively

$$\frac{\partial u}{\partial t}-\frac{\partial u}{\partial y}=\frac{\partial^2 u}{\partial y^2}+Gr\cos(\alpha)\theta+Gm\cos(\alpha)C-\left(M+\frac{1}{K}\right)u, \tag{10}$$

$$\frac{\partial\theta}{\partial t}-\frac{\partial\theta}{\partial y}=\frac{1}{\Pr}\left(1+\frac{4R}{3}\right)\frac{\partial^2\theta}{\partial y^2}+D_u\frac{\partial^2 C}{\partial y^2} \tag{11}$$

$$\frac{\partial C}{\partial t}-\frac{\partial C}{\partial y}=\frac{1}{Sc}\frac{\partial^2 C}{\partial y^2}+Sr\frac{\partial^2\theta}{\partial y^2}-K_r C \tag{12}$$

With boundary and initial condition

$$\begin{array}{llllll} t\le 0 & u=0 & \theta=0 & C=0 & \forall\, y & \\ t\ge 0 & u=1 & \theta=e^{-t} & C=e^{-t} & at & y=0 \\ u=0 & \theta\to 0 & C\to 0 & y\to\infty & & \end{array} \tag{13}$$

3. NUMERICAL SOLUTION BY FINITE ELEMENT METHOD

Finite element technique is used to solve the velocity, momentum and energy equations (10), (11) and (12) along with the boundary conditions (13).

The Galerkin expression for the differential equation (10) becomes

$$\int_{y_j}^{y_k}\left\{N^T\left[\frac{\partial^2 u^{(e)}}{\partial y^2}-\frac{\partial u^{(e)}}{\partial t}+\frac{\partial u^{(e)}}{\partial y}-Ru^{(e)}+P\right]\right\}dy=0$$

Where $N^T=\begin{bmatrix}N_j & N_k\end{bmatrix}^T=\begin{bmatrix}N_j\\ N_k\end{bmatrix}$, $R=M+\frac{1}{K}$, $P=(G_r\cos\alpha)T+(G_m\cos\alpha)C$;

Let the linear piecewise approximation solution

$$u^{(e)} = N_j(y)u_j(t) + N_k(y)u_k(t) = N_j u_j + N_k u_k$$

The element equation is given by

$$\int_{y_j}^{y_k}\left\{\begin{bmatrix} N_j' N_j' & N_j' N_k' \\ N_j' N_k' & N_k' N_k' \end{bmatrix}\begin{bmatrix} u_j \\ u_k \end{bmatrix}\right\}dy + \int_{y_j}^{y_k}\left\{\begin{bmatrix} N_j N_j & N_j N_k \\ N_j N_k & N_k N_k \end{bmatrix}\begin{bmatrix} \dot{u}_j \\ \dot{u}_k \end{bmatrix}\right\}dy - \int_{y_j}^{y_k}\left\{\begin{bmatrix} N_j N_j' & N_j N_k' \\ N_j' N_k & N_k' N_k \end{bmatrix}\begin{bmatrix} u_j \\ u_k \end{bmatrix}\right\}dy$$

$$+ \mathrm{R}\int_{y_j}^{y_k}\left\{\begin{bmatrix} N_j N_j & N_j N_k \\ N_j N_k & N_k N_k \end{bmatrix}\begin{bmatrix} u_j \\ u_k \end{bmatrix}\right\}dy = \mathrm{P}\int_{y_j}^{y_k}\begin{bmatrix} N_j \\ N_k \end{bmatrix}dy$$

Where prime and dot denotes differentiation w.r.t, 'y' and 't' respectively Simplifying we get

$$\frac{1}{l^{(e)^2}}\begin{bmatrix} 1 & -1 \\ -1 & 1 \end{bmatrix}\begin{bmatrix} u_j \\ u_k \end{bmatrix} + \frac{1}{6}\begin{bmatrix} 2 & 1 \\ 1 & 2 \end{bmatrix}\begin{bmatrix} \dot{u}_j \\ \dot{u}_k \end{bmatrix} - \frac{1}{2l^{(e)}}\begin{bmatrix} -1 & 1 \\ -1 & 1 \end{bmatrix}\begin{bmatrix} u_j \\ u_k \end{bmatrix} + \frac{R}{6}\begin{bmatrix} 2 & 1 \\ 1 & 2 \end{bmatrix}\begin{bmatrix} u_j \\ u_k \end{bmatrix} = \frac{P}{2}\begin{bmatrix} 1 \\ 1 \end{bmatrix}$$

where $l^{(e)} = y_k - y_j = h$

In order to get the differential equation at the knot x_i, we write the element equations for the elements $y_{i-1} \le y \le y_i$ and $y_i \le y \le y_{i+1}$ assemble two element equations, we obtain

$$\frac{1}{l^{(e)^2}}\begin{bmatrix} 1 & -1 & 0 \\ -1 & 2 & -1 \\ 0 & -1 & 1 \end{bmatrix}\begin{bmatrix} u_{i-1} \\ u_i \\ u_{i+1} \end{bmatrix} + \frac{1}{6}\begin{bmatrix} 2 & 1 & 0 \\ 1 & 4 & 1 \\ 0 & 1 & 2 \end{bmatrix}\begin{bmatrix} \dot{u}_{i-1} \\ \dot{u}_i \\ \dot{u}_{i+1} \end{bmatrix} - \frac{1}{2l^{(e)}}\begin{bmatrix} -1 & 1 & 0 \\ -1 & 0 & 1 \\ 0 & -1 & 1 \end{bmatrix}\begin{bmatrix} u_{i-1} \\ u_i \\ u_{i+1} \end{bmatrix} + \frac{R}{6}\begin{bmatrix} 2 & 1 & 0 \\ 1 & 4 & 1 \\ 0 & 1 & 2 \end{bmatrix}\begin{bmatrix} u_{i-1} \\ u_i \\ u_{i+1} \end{bmatrix} = \frac{P}{2}\begin{bmatrix} 1 \\ 2 \\ 1 \end{bmatrix}$$

We put the row equation corresponding to the knot 'i', is

$$\frac{1}{l^{(e)^2}}\left[-u_{i-1} + 2u_i - u_{i+1}\right] + \frac{1}{6}\left[\dot{u}_{i-1} + 4\dot{u}_i + \dot{u}_{i+1}\right] - \frac{1}{2l^{(e)}}\left[-u_{i-1} + u_{i+1}\right] + \frac{R}{6}\left[u_{i-1} + 4u_i + u_{i+1}\right] = P$$

Applying Crank-Nicholson method to the above equation then we gets

$$A_1 u_{i-1}^{n+1} + A_2 u_i^{n+1} + A_3 u_{i+1}^{n+1} = A_4 u_{i-1}^{n} + A_5 u_i^{n} + A_6 u_{i+1}^{n} + 12Pk$$

Where A_1 = -6r+2 + 3rh + Rk ; A_2 = 4Rk + 12r + 8; A_3 = 2 + Rk - 6r – 3hr;
A_4 = 2 – Rk – 3rh + 6r; A_5 = -12r+8-4Rk; A_6 = 2 – Rk + 3rh + 6r; (14)

$$P = (G_r \cos\alpha)T_i^j + (G_m \cos\alpha)C_i^j;$$

Applying similar procedure to the equation (11), then we get

$$B_1 T_{i-1}^{n+1} + B_2 T_i^{n+1} + B_3 T_{i+1}^{n+1} = B_4 T_{i-1}^{n} + B_5 T_i^{n} + B_6 T_{i+1}^{n} + 12\mathrm{kQ} \quad (15)$$

Where Q = (Pr)(Du) $\left(\frac{\partial^2 C}{\partial y^2}\right)$ and Z= $\left(1 + \frac{4R}{3}\right)$

B_1 = -6Zr+3(Pr)rh+2Pr; B_2 = 12Zr+8Pr; B_3 = -6Zr-3(Pr)rh+2(Pr);
B_4 = 6Zr-3(Pr)rh+2(Pr); B_5 = -12Zr+8Pr; B_6 = 6Zr+3(Pr)rh+2(Pr)

Applying similar procedure to the equation (12), then we get

$$J_1 C_{i-1}^{n+1} + J_2 C_i^{n+1} + J_3 C_{i+1}^{n+1} = J_4 C_{i-1}^{n} + J_5 C_i^{n} + J_6 C_{i+1}^{n} + 12\mathrm{kW} \quad (16)$$

Where W= (Sr) (Sc) $\left(\frac{\partial^2 \theta}{\partial y^2}\right)$

and J_1 = -6r+3 (Sc)rh+2Sc+KrSck; J_2 = 12r+8Sc+4KrSck; J_3 = -6r-3(Sc)rh+2Sc+KrSck;
J_4 = 6r-3(Sc)rh+2Sc-KrSck; J_5 = -12r+8Sc-4KrSck; J_6 = 6r+3(Sc)rh+2Sc-KrSck;

Here r = $\frac{k}{h^2}$ and k, h are mesh sizes along y- direction and time-direction respectively index 'i' refers to space and 'j' refers to time .The mesh system consists of h=0.1 and k=0.001.

In the equations (14), (15), and (16), taking i = 1(1)n and using boundary conditions (13), then we get the following system of equations are obtained:

$A_i X_i = B_i$ for i=1(1)n

Where A_i's are matrices of order n and X_i, B_i's are column matrices having n-components. The solutions of above system of equations are obtained by using Thomas algorithm for velocity, temperature and concentration. Also, numerical solutions for these equations are obtained by C++ program. In order to prove the convergence and stability of Galerkin finite element method, the same C++ program was run with small values of h and k no significant change was observed in the values of u, T and C. Hence the Galerkin Finite Element Method is stable and convergent.

Skin- friction

Skin-friction coefficient (τ) at the plate is

$$\tau = -\left(\frac{\partial u}{\partial y}\right)_{y=0}$$

Nusselt number (N_u) at the plate is

$$N_u = -\left(\frac{\partial T}{\partial y}\right)_{y=0}$$

Sherwood number (S_h) at the plate is

$$S_h = -\left(\frac{\partial C}{\partial y}\right)_{y=0}$$

4. RESULTS AND DISCUSSIONS

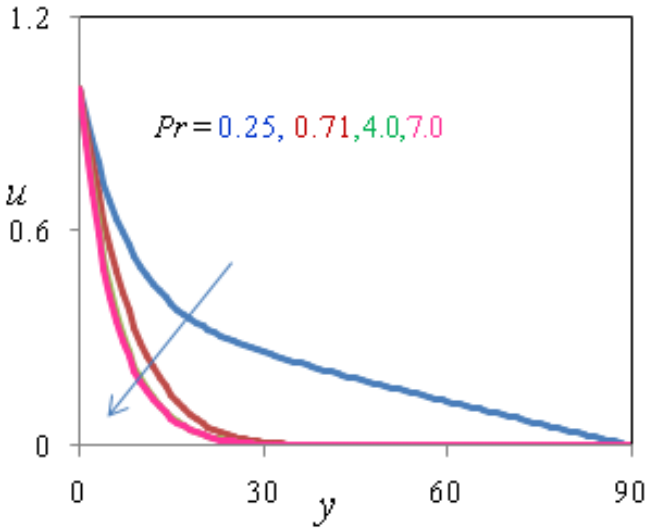

Figure 1: Velocity Profiles for different values of Pr when Gr=5, Gm=10, R=2, K=1, M=5, Sc=0.66, Du=0.7, Sr=1, α =30, t=0.2, Kr=1.0

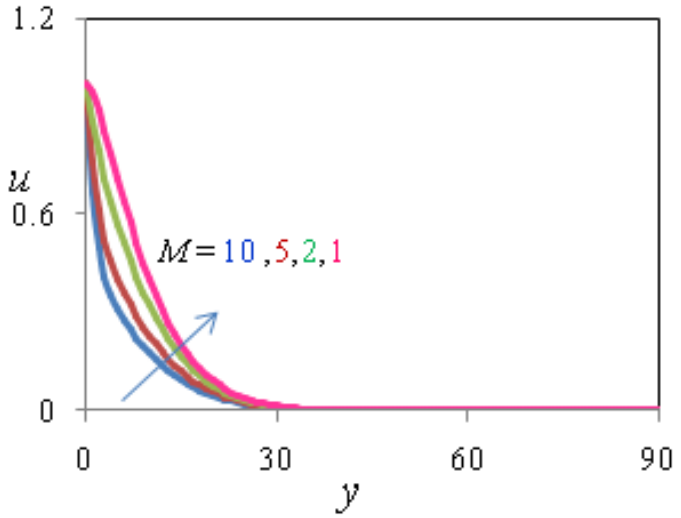

Figure 2: Velocity Profiles for different values of M, when Gr=5, Gm=10, R=2, K=1, Pr=0.71, Sc=0.66, Du=0.7, Sr=1, α =30, t=0.2, Kr=1.0

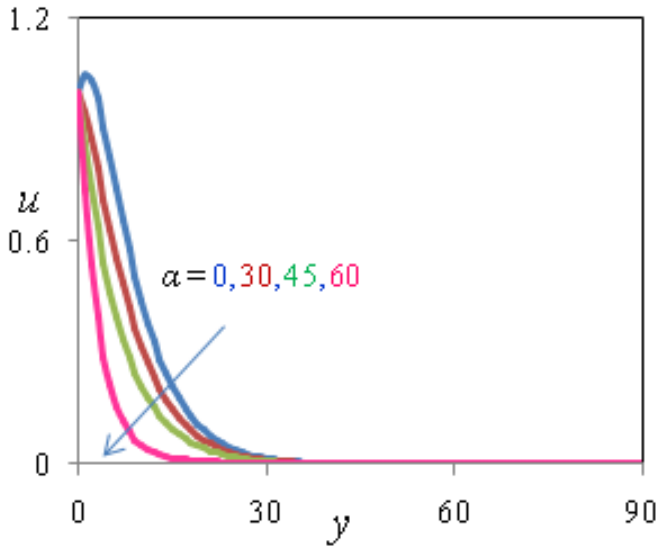

Figure 3: Velocity Profiles for different values of α when Gr=5, Gm=10, R=2, K=1, M=5, Sc=0.66, Du=0.7, Sr=1, t=0.2, Pr=0.71, Kr=1.0

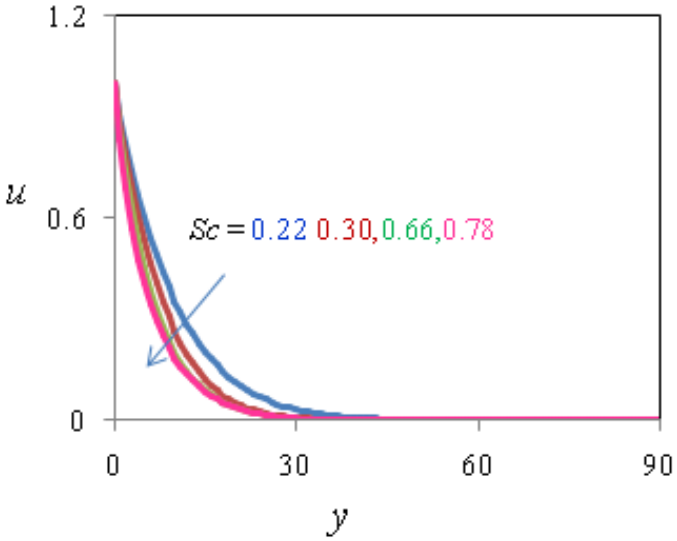

Figure 4: Velocity Profiles for different values of Sc when Gr=5, Gm=10, R=2, K=1, M=5, Pr=0.71, Du=0.7, Sr=1, α =30, t=0.2, Kr=1.0

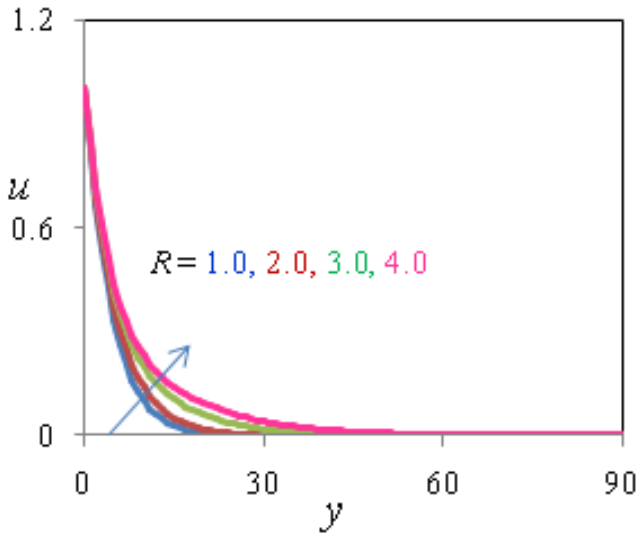

Figure 5: Velocity Profiles for different values of R when Gr=5, Gm=10, K=1, M=5, Sc=0.66, Du=0.7, Sr=1, α =30, t=0.2, Pr=0.71, Kr=1.0

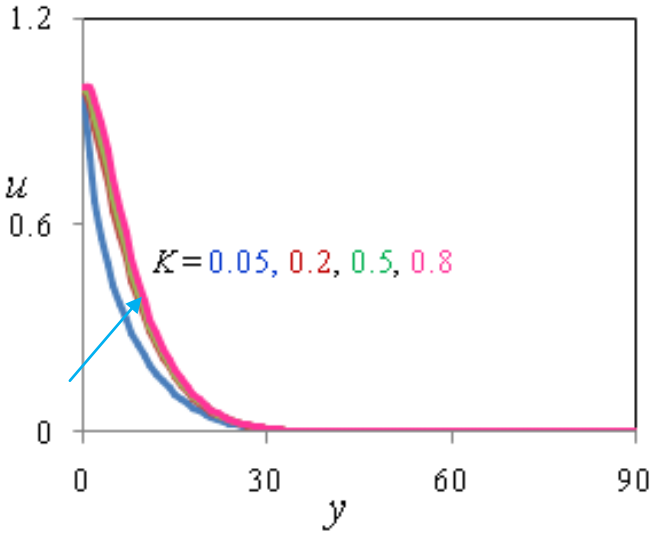

Figure 6: Velocity Profiles for different values of K when Gr=5, Gm=10, R=2, M=5, Sc = 0.66, Du=0.7, Sr=1, α =30, t=0.2, Pr=0.71, Kr=1.0

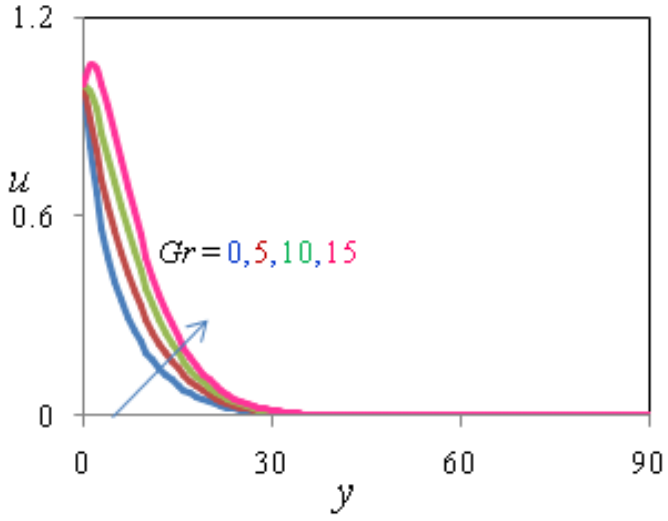

Figure 7: Velocity Profiles for different values of Gr when Gm=10, R=2, K=1, M=5, Sc = 0.66, Du=0.7, Sr=1,, t=0.2,Pr=0.71,Kr=1.0, α =30.

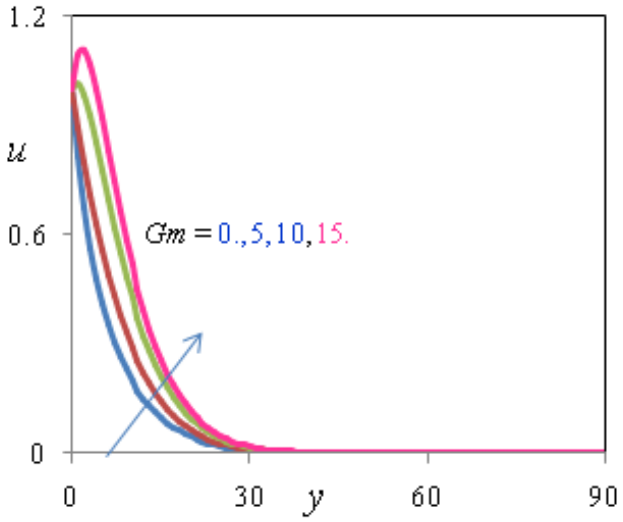

Figure 8: Velocity Profiles for different values of Gm when Gr=5, R=2, K=1, M=5, Sc=0.66, Du=0.7, Sr=1, α =30, t=0.2, Pr=0.71, Kr=1.0

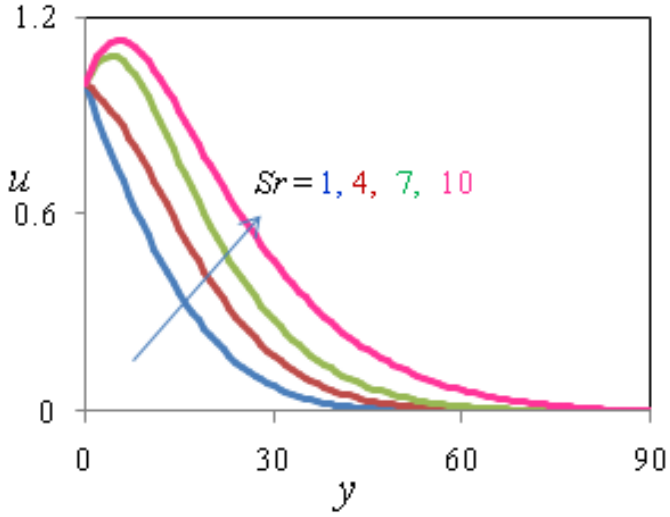

Figure 9: Velocity Profiles for different values of Sr when Gr=5, Gm=10, R=2, K=1, M=5, Sc=0.66, Du=0.7, α =30, t=0.2, Pr=0.71, Kr=1.0

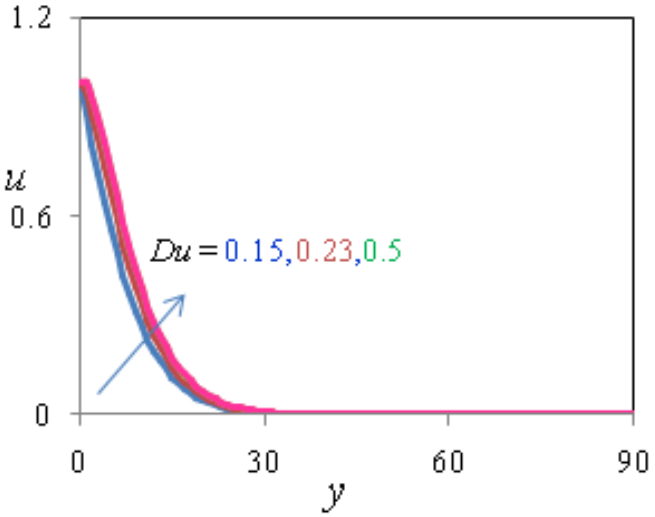

Figure 10: Velocity Profiles for different values of Du when Gr=5, Gm=10, R=2, K=1, M=5, Sc=0.66, Sr=1, α =30, t=0.2, Pr=7, Kr=1.0

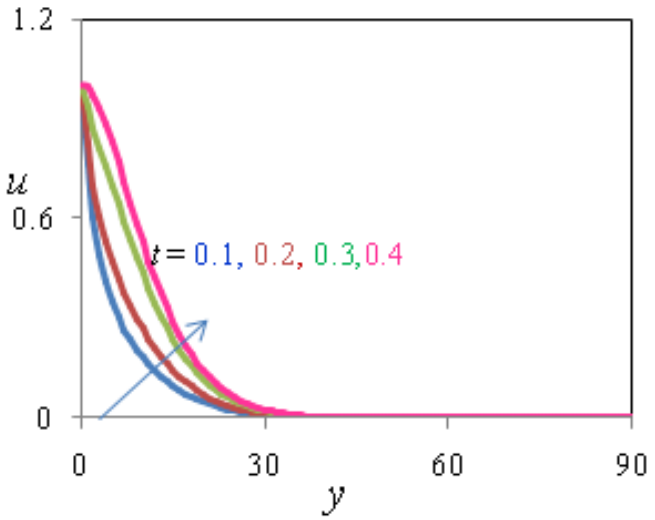

Figure 11: Velocity Profiles for different values of t when Gr=5, Gm=10, R=2, K=1, M=5, Sc=0.66, Du=0.7, Sr=1, α =30, Pr=0.71, Kr=1.0

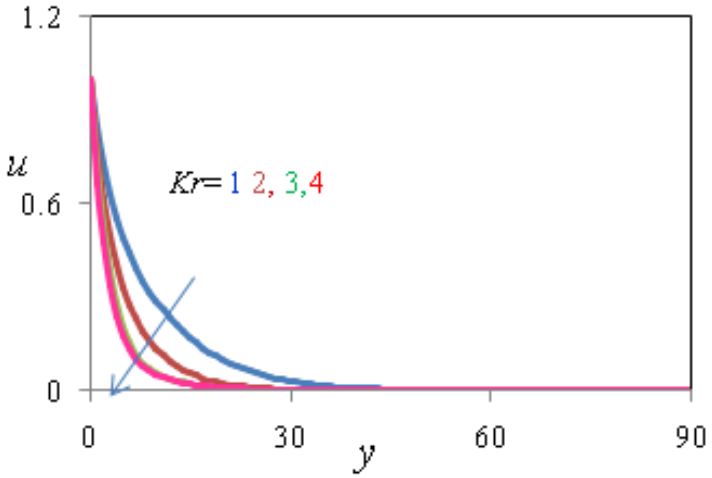

Figure 12: Velocity Profiles for different values of Kr when Gr=5, Gm=10, R=2, K=1, M=5, Sc=0.66, Du=0.7, Sr=1, α =30, t=0.2, Pr=0.71

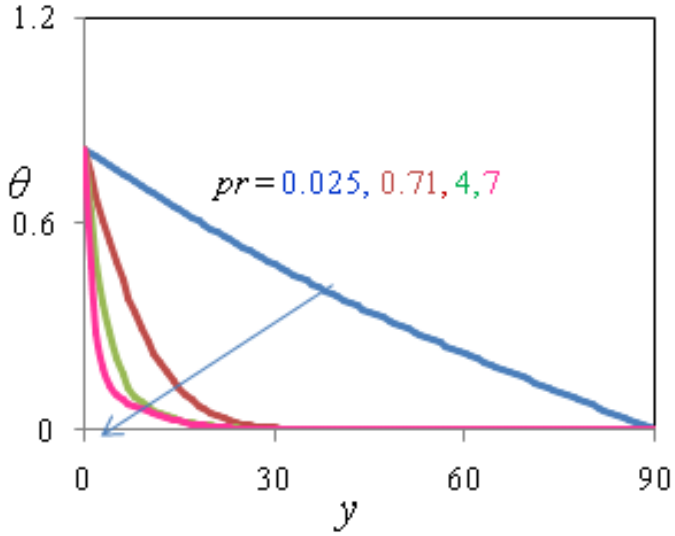

Figure 13: Temperature Profiles for different values of Pr when Gr=5, Gm=10, R=2, K=1, M=5, Sc=0.66, Du=0.7, Sr=1, α =30, t=0.2, Kr=1.0

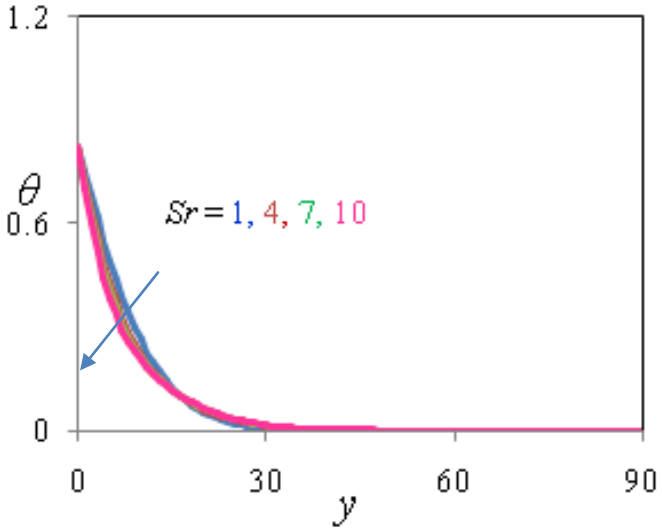

Figure 14: Temperature Profiles for different values of Sr when Gr=5, Gm=10, R=2, K=1,M=5, Sc=0.66, Du=0.7, α =30, t=0.2, Pr=0.71, Kr=1.0

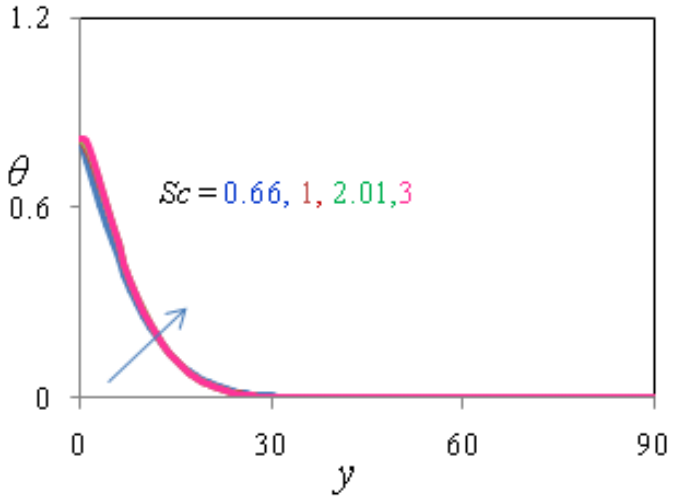

Figure 15: Temperature Profiles for different values of Sc when Gr=5, Gm=10, R=2, K=1, M=5, Du=0.7, Sr=1, α =30, t=0.2, Pr=0.71, Kr=1.0

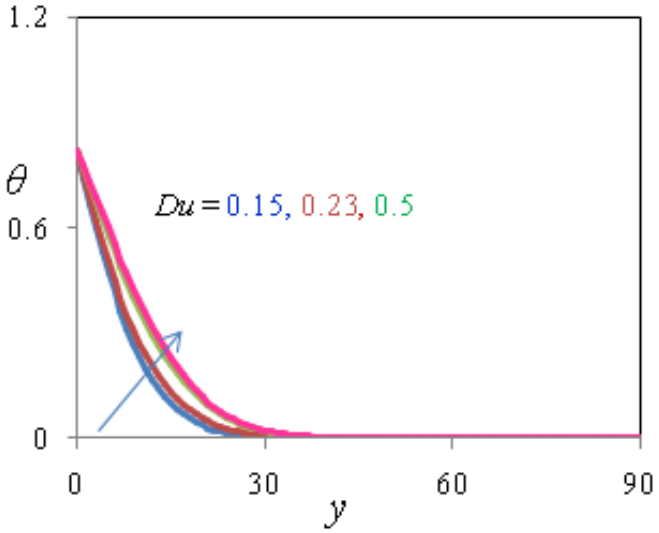

Figure 16: Temperature Profiles for different values of Du when Gr=5, Gm=10, R=2, K=1, M=5, Sc=0.66, Sr=1, α =30, t = 0.2, Pr = 0.71, Kr = 1.0

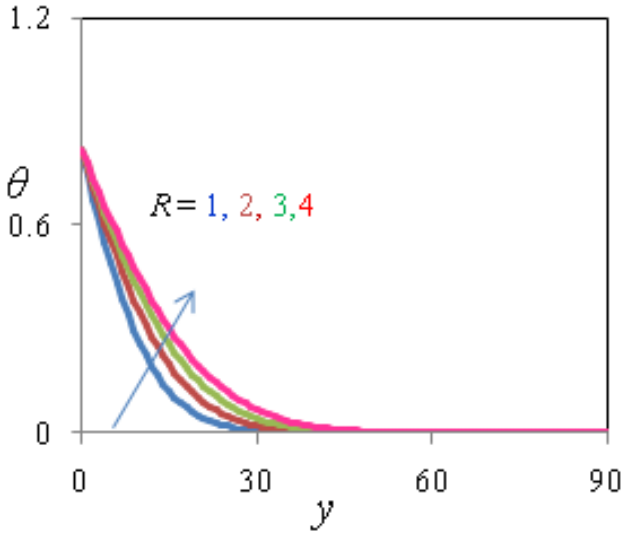

Figure 17: Temperature Profiles for different values of R when Gr=5, Gm=10, K=1, M=5, Sc=0.66, Du=0.7, Sr=1, α =30, t=0.2, Pr=0.71, Kr=1.0

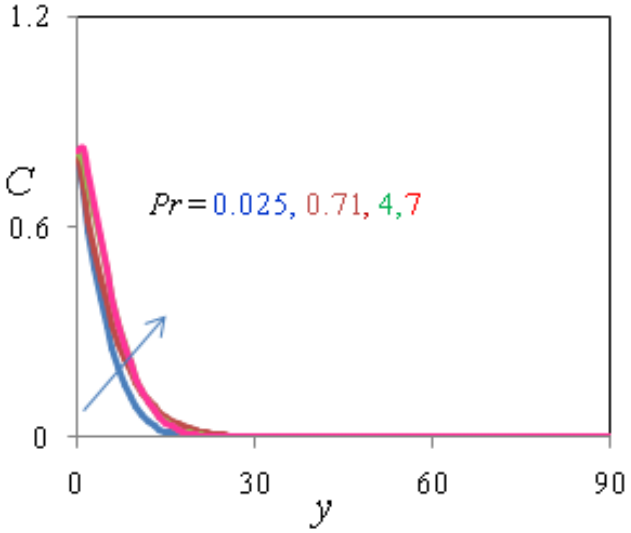

Figure 18: Concentration Profiles for different values of Pr when Gr=5, Gm=10, R=2, K=1, M=5, Sc=0.66, Du=0.7, Sr=1, α =30,t=0.2,Kr=1.0.

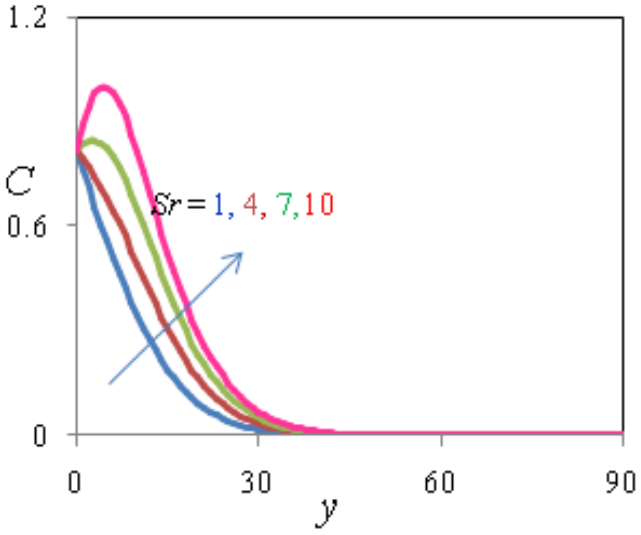

Figure 19: Concentration Profiles for different values of Sr when Gr=5, Gm=10, R=2, K=1, M=5, Sc=0.66, Du=0.7, α =30, t=0.2, Pr=0.71, Kr=1.0

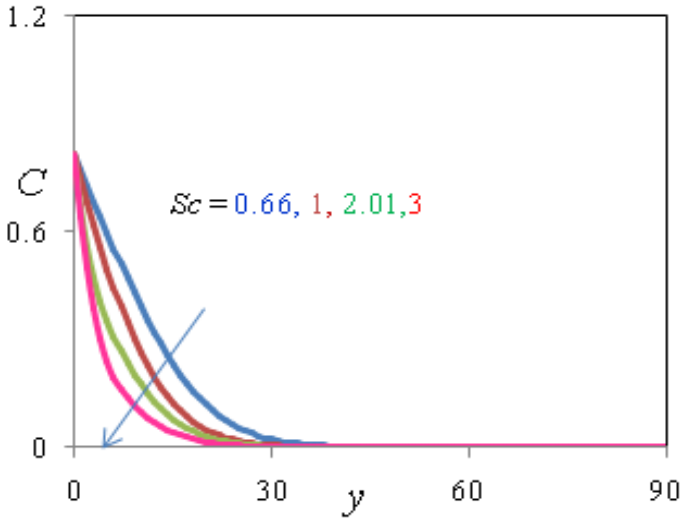

Figure 20: Concentration Profiles for different values of Sc when Gr=5, Gm=10, R=2, K=1, M=5, Du=0.7, Sr=1, α =30,t=0.2, Pr=0.71, Kr=1.0

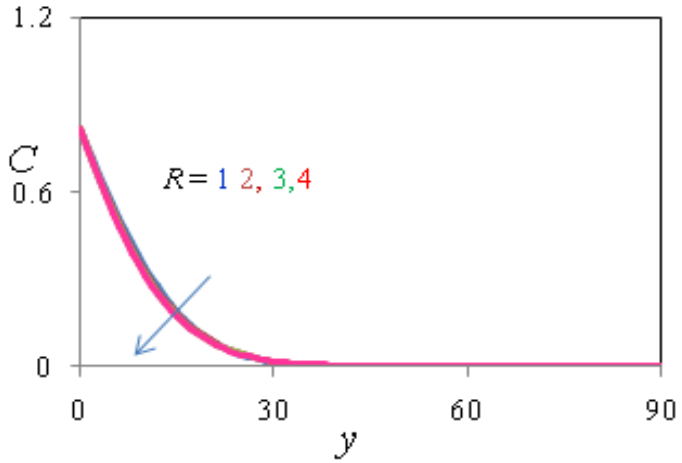

Figure 21: Concentration Profiles for different values of R when Gr=5, Gm=10, K=1, M=5,Sc=0.66, u=0.7,Sr=1, α =30,t=0.2,Kr=1.0,Pr=0.71

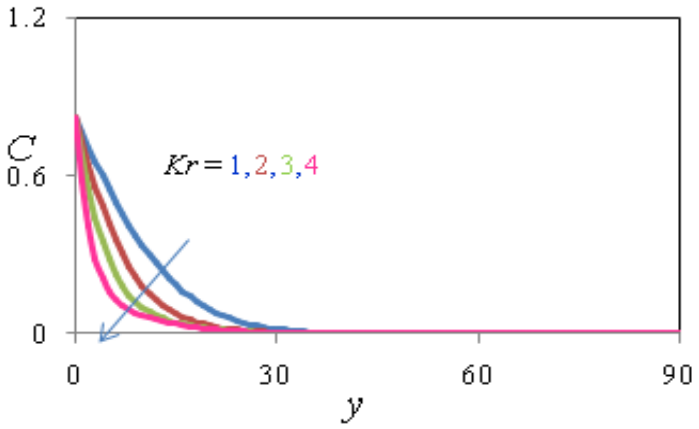

Figure 22: Concentration Profiles for different values of Pr when Gr=5, Gm=10, R=2, K=1, M=5, Sc=0.66, Du=0.7, Sr=1, α =30, t=0.2, Pr=0.71

Figures 1 to 12 depict the variation of dimensionless velocity field u against the influence of physical parameters. From the Figures 1 to 4 it is clearly observed that the effect of Prandtl number Pr, magnetic parameter M, inclination angle α and Schmidt number Sc over the velocity field u. Increase in Pr, M, Sc and α contributes to decrease in velocity. The effect of buoyancy force decreases because of multiplication factor cos (α).

For different values of radiation parameter R, permeability K, Grashof number Gr, modified Grashof number Gm, the soret number Sr, Dufour number Du, and time t, the velocity profiles are plotted from figures 5 to11.It is seen that the velocity increases as these parameters increases. It is clearly observed that the velocity profile decrease by increasing the chemical reaction parameter, shown in Figure 12.

From the figures (13) and (14) we notice that the temperature decreases as prandtl number Pr and soret number Sr increases and increasing the Schmidt number Sc and Dofour number Du, increases the temperature profile which is clearly observed from figures (15) and (16). Figure (16) reveals that temperature increases as radiation parameter R increases.

Figure (18) shows that the fluid concentration *C*, first increase rapidly then decrease on increasing the prandtl number Pr. Figure (19) depicts that concentration profile increases as soret number increases. Increasing Schmidt number *Sc*, it is analyzed that concentration field decreases in Figure (20), this causes the concentration buoyancy effects to decrease yielding a reduction in the fluid velocity. It is analyzed in figure (21) that on increasing radiation parameter *R*, and chemical reaction parameter *Kr* concentration decreases.

Table-1: Comparison of Skin-friction results (τ) with the Skin-friction results (τ^*) obtained by Pandya and Shukla [7] for different values of parameters.

t	R	Pr	M	K	Sc	Sr	α	Du	Gm	Gr	τ	τ^*
0.2	1	0.71	5	1	0.66	1	30	0.7	10	5	0.67512352	0.677699
0.2	2	0.025	5	1	0.66	1	30	0.7	10	5	0.59656721	0.596546
0.1	2	0.71	5	1	0.66	1	30	0.7	10	5	1.61783452	1.61605
0.2	1	0.71	5	1	0.66	1	30	0.7	10	10	-0.5746182	-0.57371

Table-2: Comparison of Nusselt number results (Nu) with the Nusselt number Results (Nu^*) obtained by N .Pandya and A.K. Shukla [7] for different values of parameters.

t	R	Pr	M	K	Sc	Sr	α	Du	Gm	Gr	Nu	Nu^*
0.2	1	0.71	5	1	0.66	1	30	0.7	10	5	0.71487653	0.713983
0.2	2	0.025	5	1	0.66	1	30	0.7	10	5	0.18385672	0.184229
0.1	2	0.71	5	1	0.66	1	30	0.7	10	5	0.89345645	0.892766
0.4	2	0.71	5	1	0.66	1	30	0.7	10	5	0.27345124	0.272914

Table-3: Comparison of Sherwood number results (Sh) with the Nusselt number Results (Sh^*) obtained by N.Pandya and A.K. Shukla [7] for different values of parameters.

t	R	Pr	M	K	Sc	Sr	α	Du	Gm	Gr	Nu	Sh^*
0.2	1	0.71	5	1	0.66	1	30	0.7	10	5	1.22745432	1.2275
0.2	2	0.025	5	1	0.66	1	30	0.7	10	5	0.44386123	0.44484
0.1	2	0.71	5	1	0.66	1	30	0.7	10	5	1.9336578	1.93473
0.4	2	0.71	5	1	0.66	1	30	0.7	10	5	0.7812675	0.780744

V. CONCLUSION

In this paper we have studied the chemical reaction and Dufour soret effects on MHD flow past a vertical plate with variable temperature and mass diffusion. From present numerical study the following conclusions can be drawn

1) The velocity increases with the increase of Gr and Gm.
2) The velocity decreases with increase in inclination angle
3) The velocity decreases with an increase in the magnetic parameter.
4) The velocity increases with an increase in the permeability of the porous medium parameter.
5) Increasing the prandtl number substantially decreases the velocity and the temperature profiles.
6) The velocity as well as concentration decreases with an increase in the Schmidt number.

7) The velocity as well as concentration decreases with an increase in the chemical reaction parameter
8) On comparing the Skin-friction(τ) ,Nusselt number(Nu) and Sherwood number (Sh) results with the Skin-friction results (τ^*), Nusselt number results (Nu^*) and Sherwood number results (Sh^*) of pandya and Shukla [7] from Table 1, 2 and 3, it can be seen that they agree very well.

REFERENCES

1. K.D Alagoa, G.Tay and T.M. Abbey, Radiative and free convective effects of MHD flow through a porous medium between infinite parallel plates with time dependent suction. Astrophy & space sci., 260(1999), 455-468.
2. A.C Cogley, W.C. Vincenti and S.E.Gilles, Differential approximation for radiation transfer in a non-gray gas near equilibrium. Am. Inst. Aeronaut Astronaut J.vol, 6, pp-551-555, 1968
3. Rajput U. S. and Sahu. P. K., 2011. Effects of rotation and magnetic field on the flow past an exponentially accelerated vertical plate with constant temperature, International Journal of Mathematical Archive, Vol. 2, No. 12, pp 2831-2843.
4. Soundalgekar V.M and Wavre P.D (1977): unsteady free convective flow past an infinite vertical plate with constant suction and mass transfer. Int. J. Heat and Mass Transfer, vol.19, 1363-1373
5. J. Anand Rao, P. Ramesh Babu and R. Srinivasa Raju, Finite element analysis of unsteady MHD free convection flow past an infinite vertical plate with Soret, Dufour thermal radiation and heat source. ARPN Journal of engineering and applied sciences Vol. [10], No 12 2015.
6. E.R.G Eckert, R.M Drake, Analysis of Heat and Mass Transfer, McGraw-Hill, New York 1972.
7. Z Durusukanya, W.M worek, Diffusion-thermo and thermal diffusion effects in transient and steady natural convection from vertical surface,Int. J. Heat Mass Transfer, 35(8), pp 2060-2065,1992.
8. M.S Alam, M.M Rahman, Dufour and soret effects on MHD free convective heat and mass transfer flow past a vertical flat plate embedded in a porous medium. J.Naval architecture and Marine Engineering 2(1), pp.55-65, 2005.
9. N .Pandya and A,K, Shukla, soret Dufour and radiation effects on unsteady MHD flow past an impulsively started inclined porous plate with variable temperature and Mass diffusion. Int. J. of Mathematics and Scientific Computing. (ISSN: 2231-5330) Vol. 3, No2, 2013.

Source of support: Nil, Conflict of interest: None Declared